Development of a learning phase transformation and dilatometer model for the virtual process design of press hardening processes

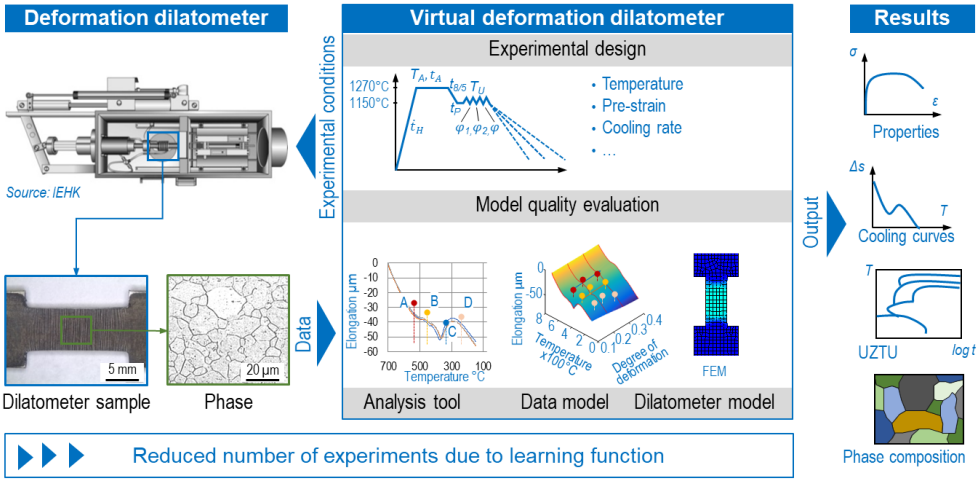

Institutes involved in the project

Chair of Hybride Manufacturing, Brandenburgische Technische Universität Cottbus-Senftenberg[1]

Institute of Manufacturing Technology, Friedrich-Alexander-Universität Erlangen-Nürnberg[2]

Founding

The research project IGF 20071 BG / FOSTA P1305 "Development of a learning phase transformation and dilatometer model for the virtual process design of press hardening processes" from the Research Association for steel Application (FOSTA), Düsseldorf, was supported by the Federal Ministry of Economic Affairs and Climate Action through the German Federation of Industrial Research Associations (AiF) as part of the programme for promoting industrial cooperative research (IGF) on the basis of a decision by the German Bundestag. The project was carried out at the Chair of Hybride Manufacturing BTU Cottbus Senftenberg and the Institute of Manufacturing Technology, FAU Erlangen.

Supported by:

Federal Ministry for Economic Affairs and Climate Action

on the basis of a decision by the German Bundestag

FOSTA Research Association for Steel Application

Contact:

[1] johannes.buhl@b-tu.de

[2] alexander.horn@fau.de

1. Introduction

Hot stamping of boron-manganese steel is a state-of-the-art process for automotive car body parts. The high relevance of hot-stamped components can be explained by the lightweight potential due to the high strength of the material after processing. In the first step, the semi-finished parts are fully austenitized above AC_3 temperature. Subsequently, for the heat treatment, the sheets are transferred to the press, formed, and simultaneously in-die quenched [1]. Because of the high cooling rates during quenching, martensitic transformation takes place, which leads to an ultimate tensile strength of at least 1500 MPa. Offering high structural integrity, hot-stamped boron-manganese steel is particularly suitable for safety-relevant components such as A- or B-pillars. However, residual elongation is limited due to the martensitic microstructure. Further improvement in passenger safety is achievable by using components having tailored properties [2]. In this context, different process variations are applied to maintain or recover more ductile phases like ferrite, pearlite, or bainite [3]. A very common approach is the implementation of differential cooling strategies. This can be realized through different techniques. One method is to reduce the heat transfer between tool and workpiece by applying tool steels with various thermal conductivity [4], grooved tools [5], or insulated tool segments [6]. Thus, the quenching rate is reduced. While the sheets in this method are still being continuously cooled until extraction, isothermal holding is applied in the case of ‘tailored tempering’. Heated tool segments are used in this process variant to ensure phase transformation above the martensite start temperature [7].

In all hot stamping processes, the evolution of the microstructure is of high relevance for the process design. Regarding conventional hot stamping, it is important to ensure that the quenching rate is sufficient for martensitic transformation. In terms of partial hot stamping processes, exact process control is necessary to guarantee the formation of the desired phase composition. For this reason, various studies have already been conducted on the phase transformation behavior of boron-manganese steels under different thermal and mechanical load conditions. In his investigations, Naderi [8] identified the critical cooling rate for the martensitic transformation of 22MnB5 to 25 K/s. As soon as pre-strain in the austenitic region is considered, the incubation time of ferrite is shortened, as seen in the work of Barcellona and Palmeri [9] or Min et al. [10]. Nikravesh et al. [11] observed an increase of 40 K/s in the critical cooling rate after 40% of compression. If deformation is applied simultaneously to quenching, the amount of martensite is reduced as well [12]. In the work of Abbasi et al. [13], the effect of isothermal as well as non-isothermal deformation was investigated. In the case of isothermal deformation at austenitization temperature, samples exhibited a fully martensitic microstructure, while other phases were apparent for simultaneously quenched and deformed specimens. As concluded by Matsumoto et al. [14], the reduction of martensite increases with decreasing deformation temperature. In the case of the bainitic transformation, the effect of the pre-strain is influenced by the cooling rate.

An accurate prediction of these microstructural changes along the process chain is required for a time- and cost-efficient process design. This requires respective material models to simulate the phase transformation kinetics. Currently, this is only possible by conducting a large number of time-consuming dilatometer tests. Therefore, within the research project FOSTA P1305 / IGF 20071 BG, a virtual dilatometer was developed to reduce experimental effort and to improve the design of hot stamping processes.

2. Materials and Methods

2.1 22MnB5

The tests within the scope of the completed research project were carried out with the boron-manganese steel 22MnB5. In the as-received condition, the microstructure is ferritic-pearlitic, with an initial hardness of around 180 HV [15]. The tensile strength is in the range of 500 MPa to 700 MPa, with about 12% elongation at break [16]. Following the press hardening process, strengths of 1500 MPa are usually achieved with a reduced elongation at break of 5%. The hardness is more than 470 HV [16].

2.2 Materials characterization

The study of solid-state phase transformation coupled with the application of plastic strain is performed using a Bähr DIL 805 A/D/T forming dilatometer. In dilatometry, the sample of 22MnB5 is heated in a controlled manner at a defined heating rate, held at an austenitizing temperature for 300 s, and then cooled to the desired forming temperature at 30 K/s. After plastic straining has been performed at a defined strain rate, the specimen is cooled to room temperature in a controlled manner at the desired cooling rate. For this purpose, a thermocouple is welded to the surface in the center of the specimen.

The dilatometer experiments are the basis for describing the material's behavior. Further characterization techniques are utilized to investigate the resulting mechanical properties. These are uniaxial tensile tests, microhardness measurements according to Vickers, and metallographic analysis.

To validate the findings and the material model developed, sample components are pressed off under realistic conditions. The geometry corresponds to a simplified B-pillar. As one focus of the research project was on the process route of partial press hardening, a locally heatable tool was used.

3. Setting up a data basis for the virtual dilatometer

3.1 Investigated parameters

For the extension of a material model, it is necessary to first create a comprehensive data basis through extensive transformation experiments. The subjects of the investigations are the two process routes of continuous quenching with variable quenching rate and isothermal holding at varying holding temperatures. In both process routes, uniform austenitization is carried out first. For this purpose, the samples are heated to T_a = 950 °C at 5 K/s and then held for 5 min. This is followed by cooling to R_1 = 800 °C at a cooling rate of 30 K/s. In the real process, this corresponds to the transfer between a furnace and a forming press. At 800 °C, potential forming also takes place to the degree of deformation φ with the strain rate $\dot{\phi}$. In the continuous quenching process route, different cooling rates $\dot{T}_k$ between 5 and 50 K/s are then applied, and the sheets are cooled to room temperature. In isothermal holding, cooling is first carried out at 50 K/s to the target temperature T_I between 800 °C and 450 °C, followed by a holding time t_I of up to 200 seconds.

3.2 Transformation rate

Following the dilatometer tests, the measurement results were evaluated. With the help of the dilatation curve, transformation points were determined and the transformation kinetics were calculated. Figure 1 shows the resulting transformation rate as the main experimental result. Based on the different peaks, the individual phase transformations can be identified. For example, in the case of continuous quenching, it can be seen that a peak forms in the temperature range just below 400 °C when the quenching rate is greater than 10 K/s. This is the peak of the martensitic transformation. This corresponds to the martensite transformation.

The peak at temperatures between 650 °C and 450 °C, which is mainly a sign of ferrite and bainite, becomes continuously smaller with increasing cooling speed.

In the case of isothermal holding, the transformation rate is pictured as a function of the holding time and the holding temperature. It can be seen that the incubation of phase transformation takes longer at higher temperatures. Furthermore, the peak is smaller and is distributed over a longer duration. At lower temperatures, the phase transformation occurs much faster after reaching the isothermal holding temperature.

The transformation rate is an efficient way of storing the results from dilatometer testing. In addition, it is possible to trace back the initial dilatation curve from the transformation rate.

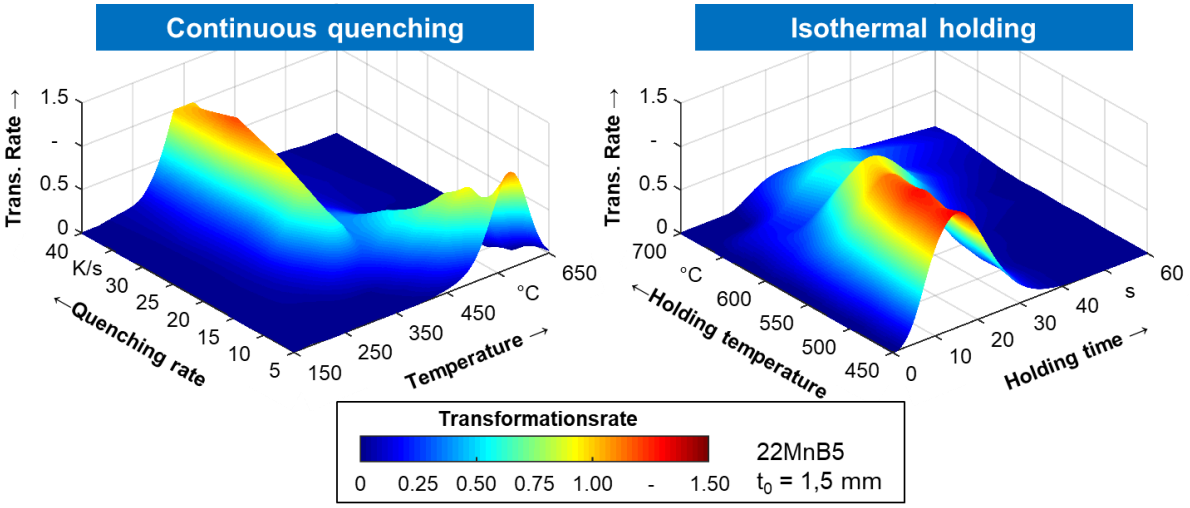

Figure 1: Transformation rate as a function of process parameters

3.3 Mechanical properties

In addition to the transformation rate, the mechanical properties in the quenched condition were also investigated. Figure 2 shows the resulting hardness values. As expected, the hardness directly correlates with the quenching rate. An increase in the quenching rate simultaneously leads to an increase in hardness. At the same time, it can be seen that at an intermediate quenching rate, the standard deviation is also increased. This is due to the formation of a mixed microstructure, as can be confirmed from the optical microscopy images. While a primarily ferritic microstructure is present at low quench rates, the proportion of bainite increases with higher cooling rates. For high quench rates, a completely martensitic microstructure is obtained.

In the case of isothermally held sheets, it can be seen that both the hardness and the tensile strength initially decrease at lower holding temperatures. At a sufficiently high holding temperature, hard phases such as bainite or martensite are still formed during subsequent quenching from the isothermal holding temperature to room temperature. If the holding temperature is reduced, the proportion of ferritic and pearlitic phases will increase. When the temperature is lowered further, both the hardness and the tensile strength start to increase again. This is due to the formation of bainitic phase fractions.

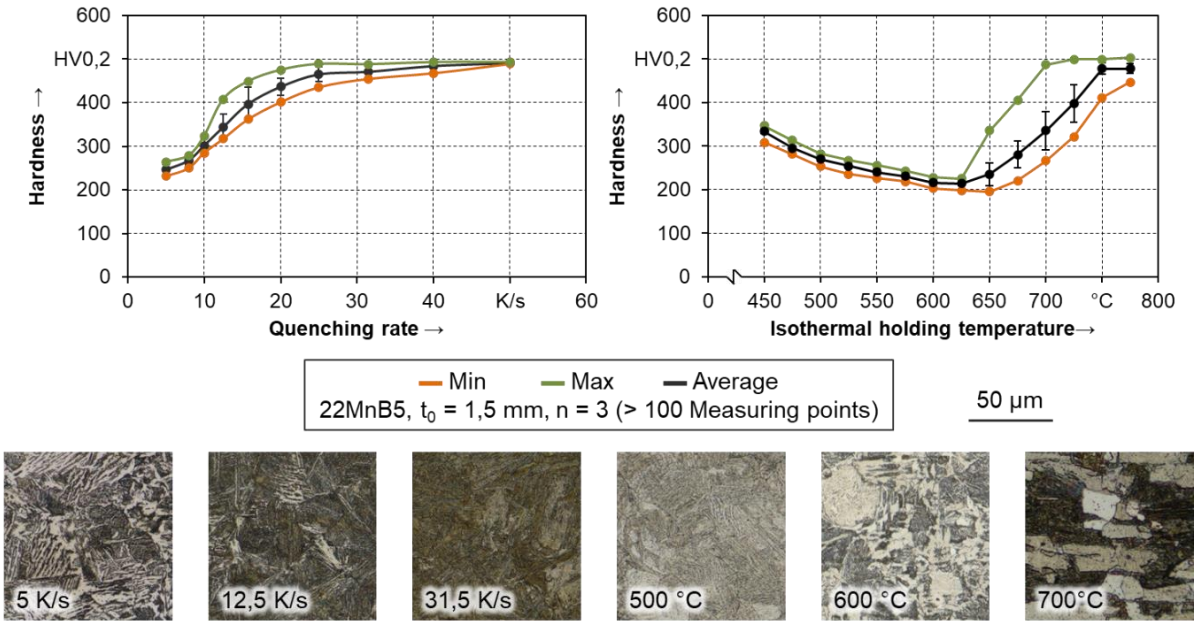

Figure 2: Hardness obtained after continuous quenching or isothermal holding, with additional micrographs

3.4 Phase transformation behavior

The phase transformation kinetics of all isothermal experiments is then used to construct the CCT diagram as shown in Figure 3. The result from the CCT diagram shows that the phase transformation is faster as the holding temperature is decreased. For example, it takes about 20 s for austenite to transform to 0.7 at the holding temperature of 550 °C, while it takes 40 s for austenite to transform to the same amount at the holding temperature of 650 °C. The hardness values at 700 °C and 725 °C are very high because the ferrite equilibrium temperature at these temperatures is around 0.30 to 0.40.

Therefore, the austenite is transformed into martensite during the subsequent cooling process. The hardness values are lower until the holding temperature reaches 600 °C. After that, the hardness values increased as the holding temperature was decreased. Further results on the phase transformation behavior and its specific modeling will be presented in future publications by the authors.

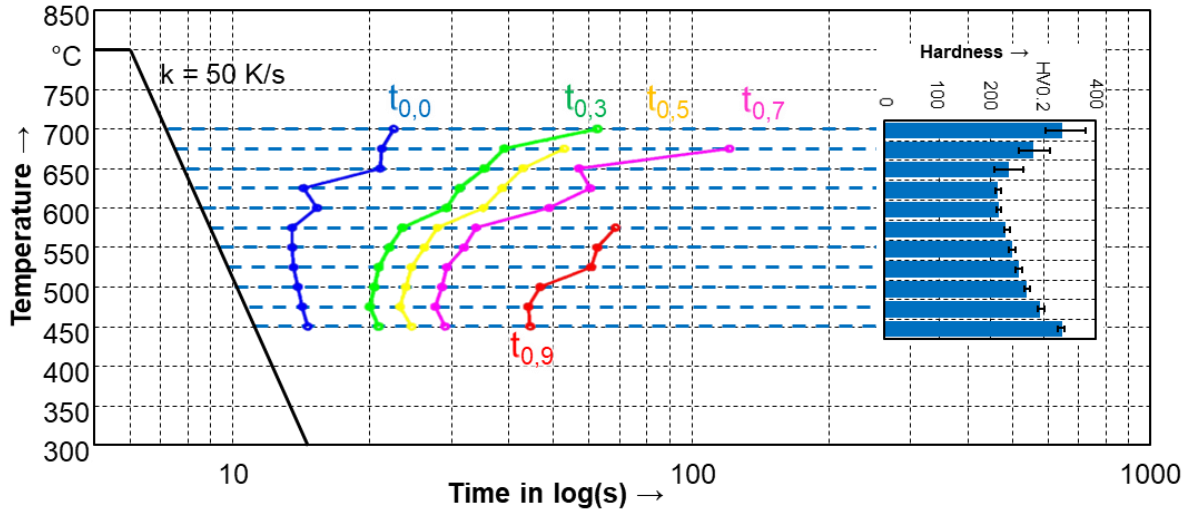

Figure 3: CCT diagram of the isothermal experiment for isothermal processing.

4. Integration of a learning function

For industrial use, it must be ensured that the calibration of the material model can be carried out with as few tests as possible. For this purpose, the experimental conditions are not specified in advance but are iteratively adjusted depending on the experimental results. This should enable the model to learn its parameters automatically. For this purpose, only a small number of experimental conditions are initially selected at the beginning of the model calibration. The algorithm will determine whether and which additional experiments will be performed in order to achieve a given model accuracy.

The "sequential improvement method" shown in Figure 4 is a statistical procedure for estimating optimal new test conditions and the expected gain in model quality. The procedure of this method is explained in the following. In the beginning, the process window is defined and the possible test conditions are constructed using Latin Hypercube Sampling (LHS). The number of initial LHS samples is chosen based on user preference, but it must be greater than the maximum number of trials.

Initially, five output sampling points are selected. These five experiments are mapped with metamodels using long-term short-term memory (LSTM). In each test condition, ten LSTM models are trained by randomly selecting the training and test sets. The training-to-testing ratio is set at 70/30.

After the training, a statistical evaluation of the metamodels is performed and a loss map is generated. After the statistical evaluation, a search algorithm is run to find a new optimal test condition based on a loss map and the LHS.

Once the experimental database has been expanded, the data model must be changed and the estimation of the model parameters repeated. This procedure is repeated until a maximum permissible error value in the entire space of experimental conditions (error sum of squares < default value) is undercut. A key challenge here is that the iterative experimental design implemented here must be combined with the identification of dependencies of the model parameters. Through the iterative experimental design, the algorithm should identify an optimal model in a learning process while keeping the number of necessary experiments for parameter determination as low as possible. As a result, the causes of the discovered dependencies can be tested for plausibility and conclusions drawn for the extension of physical model approaches.

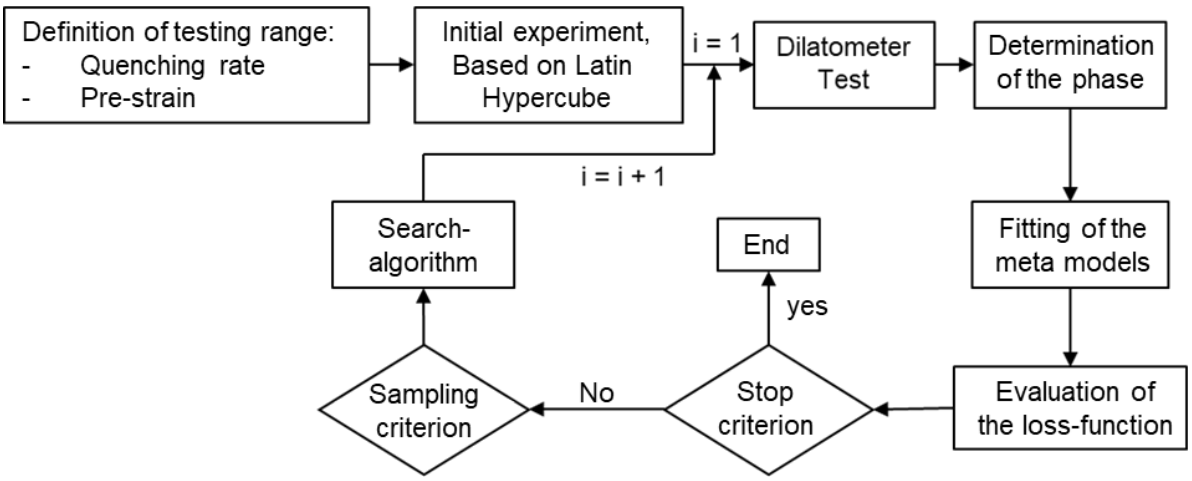

Figure 4: Sequential improvement method.

5. Transfer to other process routes

In the following investigations, the transferability of the virtual dilatometer to the application of alternative process routes is to be demonstrated. This includes, on the one hand, the prediction of the dilatation curve and, on the other hand, the prediction of the resulting mechanical properties in the form of hardness. Figure 5 shows an example of an alternative process route in which intermediate cooling is followed by renewed heating for a short time, for example in the form of a second furnace. In the tests carried out, the sheets were first cooled to a temperature of 450 °C, which is above the martensite starting temperature. Temperatures between 600 °C and 950 °C were experimentally mapped during subsequent heating. The results show that a good prediction quality of the virtual dilatometer can be achieved for all expressions of T_{heat}. It can be seen that both the first section of the quenching, as well as the intermediate heating and the final quenching, can be represented well.

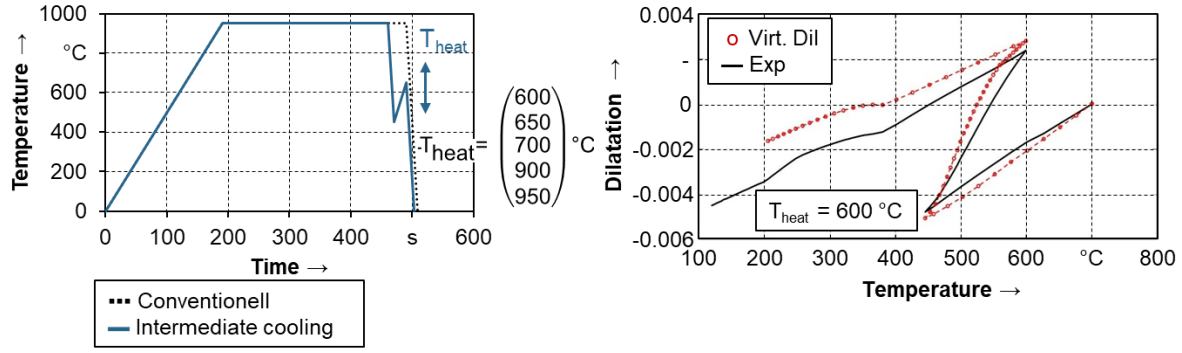

Figure 5: Exemplary process route for investigation of the transferability and predicted dilatation curve.

Besides the dilatation, the virtual dilatometer is also capable of predicting the mechanical properties. To validate the transferability of this feature, the properties of the alternate process route shown in Figure 5 were also predicted. Table 1 shows the results in comparison with experimentally evaluated properties.

Based on the curves in Figure 5, it is evident that the presented alternative process route can be predicted with high accuracy by the virtual dilatometer. The determined hardness values in Table 1 show a similar result. Within the standard deviation of the experimentally measured values, there is a good agreement with the values of the virtual dilatometer.

Table 1: Experimental and predicted hardness after processing with a different process route.

Hardness HV0.2	**600 °C**	**650 °C**	**700 °C**	**900 °C**	**950 °C**
Experiment	328 ± 29	300 ± 25	287 ± 22	482 ± 15	487 ± 11
Virtual Dilatometer	314	309	304	496	496

6. Validation of the process model with a demonstrator component

6.1 Analysis of the mechanical properties of the hot-stamped demonstrator component

For the validation of the material model, a demonstrator component with tailored properties was hot stamped. The lab-scaled b-pillar has a soft zone in its bottom part and a hard zone in its upper area. The tool temperature of the heated segment was 500 °C, while the rest of the tool was chilled with internal water cooling. The in-die quenching time after forming was 9 s. The hardness of the component was analyzed in the cross-section in the length direction.

In Figure 6, it can be seen that different mechanical properties are present in the actively heated and actively cooled areas. Analogous to the tensile strength, lower hardness values are obtained in the heated area, i.e., x < 80 mm. The lowest hardness is present in the flange and the frame and is around 250 HV0.2. Due to the spacing of the blank holder, macroscopic gaps form in the area of the flange between the workpiece and the two heated die elements, the die, and the blank holder. This delays the cooling process. Due to the drawing gap of 3 mm, a sheet thickness of 1.5 mm in the flange also results in a gap on both sides, which leads to a lower quenching rate. In the base, on the other hand, there is metallic contact on both sides. However, compared to the actively cooled zone, i.e., x > 80 mm, the critical quenching rate is significantly undercut. In the range of 35 < x < 65, a uniform hardness of about 330 HV0.2 is obtained. The microscopy image of the etched microstructure indicates a predominantly bainitic microstructure. From there, the hardness increases continuously up to a value of 530 HV0.2, which is in good agreement with the prevailing martensitic microstructure. In connection with the continuous increase in hardness, it can be seen that very high hardness values of about 480 HV0.2 have already been reached in the area of the tool parting, i.e., x ≈ 80 mm. On the workpiece side, however, the transition zone is shifted by a few millimeters into the actively heated area. On the active mold cooling side, sufficiently high quench rates are also achieved in the frame and flange to achieve the highest possible hardness values.

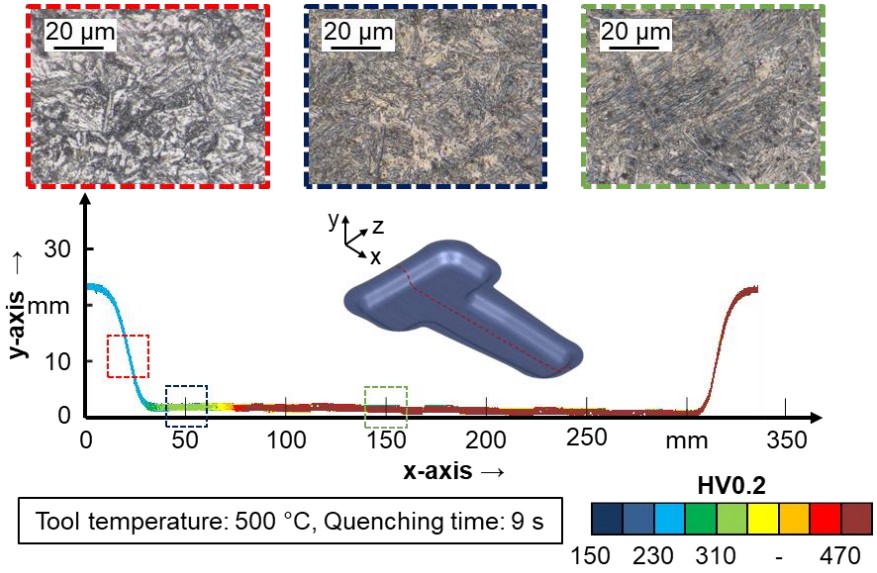

Figure 6: Resulting microhardness in the area of heated tool segments.

6.2 Validation of the process model

To validate the process model, thermomechanical load paths are taken from the simulation at different points in the area of the soft zone and the transition zone. The load paths are then used to calculate the resulting hardness values.

The result of the prediction is shown in Figure 7 in comparison with the experimental values taken from Figure 6. From the diagram, good agreement between the experimental and predicted values can be seen. In particular, the transition from the flange to the soil area, i.e. x > 20 mm, is shown well. The continuous increase in hardness at the bottom of the component is also well predicted by the material model. In the transition zone, 60 mm < x < 90 mm, a deviation between prediction and experiment is noticeable. While the slope of the curve and the final values agree well, the slope starts much earlier for the sample component. However, this circumstance can be easily explained based on the procedure for determining the hardness values. For the metallographic preparation, the sample component was separated

into several segments. For the subsequent hardness measurement, a minimum distance to the edge must then be taken into account. This distance leads to a certain uncertainty in the calculation of the absolute x-coordinate. In Figure 7, this circumstance is marked by the bars for the standard deviation in the x-direction.

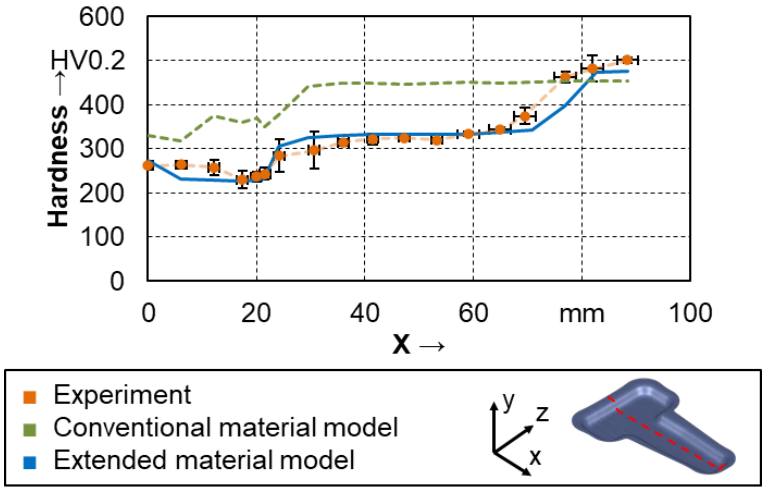

Figure 7: Comparison of predicted hardness and experimental hardness in the soft zone and the transition zone.

7. Summary

The mechanical properties of press-hardened components are significantly influenced by the final phase composition. This applies in particular to process variants in which locally varying properties are desired. Extensive knowledge of the phase transformation kinetics is therefore required for numerical process design. As a rule, the experimental investigation of the behavior of the transformation involves a large number of dilatometer tests. Particularly in the SME sector, there is often a lack of personnel with sufficient materials science expertise or the necessary experimental equipment. The primary goal of the research project was to use a physically-based model to reduce the effort required for the process design of conventional and partial press hardening processes.

First of all, a comprehensive database was created regarding the transformation behavior of the press hardening alloy 22MnB5. In this context, two process routes were considered. In addition to continuous quenching with a variable cooling rate, isothermal holding was also investigated experimentally. The dilatometer experiments were evaluated with respect to transformation temperatures and kinetics. Another aspect of building up the database was the characterization of the mechanical properties in the quenched state. For this purpose, tensile tests and hardness measurements were carried out. The results were correlated using qualitative analyses of phase composition using metallographic methods.

An existing material model was then extended based on the experimental results. The procedure as well as the detailed results will be published in further work in the future.

To reduce the experimental effort in the design of press hardening processes, another focus of the research project was the development of a learning function for iterative experimental design. The individual components, i.e., the advanced material model and the learning function for iterative test planning, were largely integrated into a graphical user interface. The corresponding tool allows the user to calculate the final phase fractions and properties based on a calibrated model. The iterative design of experiments can be used to calibrate the material model for new alloys.

The transferability of the applicability of this virtual dilatometer was demonstrated using other industrially relevant process routes. Another aspect was the validation of the process model by the partial press hardening of a sample component. Secondary samples were examined in this context, and good agreement was found between predicted and experimentally determined properties.

8. Literature

[1] Mori, K. et al.: Hot stamping of ultra-high strength steel parts. In: CIRP Ann. 66 (2017) No. 2, pp. 755-777.

[2] Maikranz-Valentin, M. et al.: Components with Optimised Properties due to Advanced Thermo-mechanical Process Strategies in Hot Sheet Metal Forming. In: Steel Res. Int. 79 (2008) No. 2, pp. 92-97.

[3] Merklein, M. et al.: Hot stamping of boron steel sheets with tailored properties: A review. In: J. Mater. Process. Technol. 228 (2016) pp. 11-24.

[4] Casas, B. et al.: Tailor made tool materials for thepresent and upcoming tooling solutions in hot sheet metal forming. In: K. Steinhoff, M. Oldenburg, B. P. (Hrsg.): Tagungsband 1st International Conference on Hot Sheet Metal Forming of High-Performance Steel - CHS², 2008, 22-36

[5] Mori, K.; Okuda, Y.: Tailor die quenching in hot stamping for producing ultra-high strength steel formed parts having strength distribution. In: CIRP Ann. 59 (2010) No. 1, pp. 291-294.

[6] Kolleck, R.; Veit, R.: Möglichkeiten zur lokalen Beeinflussung der Bauteilfestigkeit beim Presshärten. In: M. Merklein (Hrsg.): Tagungsband 3. Erlanger Workshop Warmblechumformung, Meisenbach, 2008, 65-72

[7] Bardelcik, A. et al.: A Mechanical, Microstructural, and Damage Study of Various Tailor Hot Stamped Material Conditions Consisting of Martensite, Bainite, Ferrite, and Pearlite. In: Metall. Mater. Trans. A 49 (2018) No. 4, pp. 1102-1120.

[8] Naderi, M.: Hot stamping of ultra high strength steels. Dissertation, RWTH Aachen, 2007

[9] Barcellona, A.; Palmeri, D.: Effect of Plastic Hot Deformation on the Hardness and Continuous Cooling Transformations of 22MnB5 Microalloyed Boron Steel. In: Metall. Trans. A 40 (2009) No. 5, pp. 1160-1174.

[10] Min, J. et al.: On the ferrite and bainite transformation in isothermally deformed 22MnB5 steels. In: Mater. Sci. Eng., A 550 (2012) pp. 375-387.

[11] Nikravesh, M. et al.: Influence of hot plastic deformation and cooling rate on martensite and bainite start temperatures in 22MnB5 steel. In: Mater. Sci. Eng., A 540 (2012) pp. 24-29.

[12] Naderi, M. et al.: The effects of non-isothermal deformation on martensitic transformation in 22MnB5 steel. In: Mater. Sci. Eng., A 487 (2008) No. 1-2, pp. 445-455.

[13] Abbasi, M. et al.: Isothermal versus non-isothermal hot compression process: A comparative study on phase transformations and structure–property relationships. In: Materials & Design 45 (2013) pp. 1-5.

[14] Matsumoto, T. et al.: An Investigation of Deformation Effects on Phase Transformation in Hot Stamping Processes. In: SAE International Journal of Materials and Manufacturing 9 (2016) No. 2, pp. 501-505.

[15] Geiger, M. et al.: Basic Investigations on the Hot Stamping Steel 22MnB5. In: Advanced Materials Research 6-8 (2005) pp. 795-804.

[16] https://www.thyssenkrupp-steel.com/en/products/sheet-coated-products/manganese-boron-steel-for-hot-forming/mbw-manganese-boron-steel-for-hot-forming/, (aufgerufen am 05.03.2020)